NATIONAL ADVISORY COMMITTEE FOR AERONAUTICS

TECHNICAL NOTE

No. 1788

FLIGHT TESTS OF AN APPARATUS FOR VARYING DIHEDRAL EFFECT IN FLIGHT

By William M. Kauffman, Allan Smith,
Charles J. Liddell, Jr., and George E. Cooper

Ames Aeronautical Laboratory
Moffett Field, Calif.

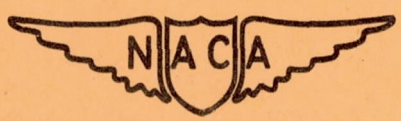

December 1948

NATIONAL ADVISORY COMMITTEE FOR AERONAUTICS

TECHNICAL NOTE NO. 1788

FLIGHT TESTS OF AN APPARATUS FOR VARYING DIHEDRAL EFFECT IN FLIGHT

By William M. Kauffman, Allan Smith,
Charles J. Liddell, Jr., and George E. Cooper

SUMMARY

A new apparatus for varying the effective dihedral in flight by means of servo actuation of the ailerons in response to sideslip angle is described. The results of brief flight tests of the apparatus, made on a conventional fighter plane for the purpose of evaluating the apparatus, are presented and discussed. The apparatus is shown to have satisfactorily simulated effective stick-fixed dihedral angles ranging from 14.9° to -2.7° under static and dynamic conditions. It is shown that the effects of a small amount of servo lag are measurable when the apparatus is simulating small negative dihedral angles during abrupt rudder kicks; however, these effects were not considered by the pilots to give the airplane an artificial feel. It appears that, with suitable minor modifications, an even wider range of dihedral may be simulated.

INTRODUCTION

The Ames Aeronautical Laboratory currently is conducting an investigation of the dynamic-stability characteristics of airplanes at cruising and high airspeeds. As part of this program, flight tests have been planned to determine the effects of changes in the static-directional-stability and static-lateral-stability parameters C_{n_β}, the rate of change of yawing-moment coefficient with sideslip, and C_{l_β}, the rate of change of rolling-moment coefficient with sideslip, on the dynamic-stability and gun-platform characteristics of a conventional fighter airplane.

A means of varying C_{n_β} and C_{l_β} in flight was considered highly desirable for this investigation in order to isolate the

effects of changes in these stability parameters on the dynamic behavior of the airplane from those due to other important influences, such as air gustiness and piloting technique. Variations of C_{n_β} and C_{l_β} ordinarily are obtained by changes in the vertical-tail area and the wing dihedral angle, respectively. Although complex mechanical systems for producing these alterations in flight could be designed, this method was not considered practicable on the test airplane. A more flexible method in which C_{n_β} and C_{l_β} are varied artificially by means of servo actuation of the main or auxiliary control surfaces in response to sideslip signals was then considered. The general principle involved has been discussed by Morgan in reference 1, in which mention is made of applications by the Germans to change the apparent longitudinal stability of a large flying boat and by the British to increase the directional damping of a dive bomber. This method appears to offer great promise, not only as a research tool but as a means of determining the optimum stability characteristics of prototypes and improving the stability characteristics of production airplanes. As a first step in applying this method to the current dynamic-stability program, an apparatus for varying the lateral-stability derivative C_{l_β} of the test airplane to include the range encountered with conventional, straight-wing configurations has been developed. Recent studies of airplane configurations involving highly swept or triangular plan forms have led to interest in the even wider range of dihedral effect which is characteristic of such plan forms. Extension of the current investigation to cover a larger range of dihedral effect and airspeed to study such factors as the maximum safe or feasible positive dihedral effect at high lift coefficients and negative dihedral effect at low lift coefficients is contemplated.

A description of the apparatus and the results of the first flight tests made for the purpose of determining its ability to simulate changes of C_{l_β} under steady and dynamic flight conditions are presented in this report.

SYMBOLS

V	true airspeed, feet per second
Vi	indicated airspeed, miles per hour
q	dynamic pressure pounds per square foot
S	wing area, square feet

b	wing span, feet
p	rolling velocity, radians per second
F	lateral stick force, pounds
P	period of lateral oscillation, seconds
$C_{\frac{1}{2}}$	number of cycles for lateral oscillation to damp to one-half amplitude
β	angle of sideslip, degrees
θ	lateral stick deflection, degrees
δ_a	total aileron deflection (sum of left and right aileron deflections, left when left aileron is up), degrees
δ_r	rudder deflection, degrees
δ_t	aileron tab deflection (positive when tab located on left aileron is up), degrees
Γ_e	effective wing dihedral angle, degrees
C_l	rolling-moment coefficient (rolling moment/qSb)
C_n	yawing-moment coefficient (yawing moment/qSb)
C_{l_β}	rate of change of rolling-moment coefficient with angle of sideslip ($\partial C_l/\partial\beta$), per degree
C_{n_β}	rate of change of yawing-moment coefficient with angle of sideslip ($\partial C_n/\partial\beta$), per degree
C_{l_p}	rate of change of rolling-moment coefficient with wing-tip helix angle $\left(\partial C_l/\partial\frac{pb}{2V}\right)$
C_{l_δ}	rate of change of rolling-moment coefficient with aileron deflection ($\partial C_l/\partial\delta_a$), per degree
$(\partial\delta_a/\partial\beta)_s$	aileron servo-gearing ratio
$(d\delta_t/d\delta_a)_s$	aileron tab servo-gearing ratio

$\left(\Delta C_{l_\beta}\right)_s$ change in C_{l_β} due to servo action

DESCRIPTION OF APPARATUS

Test Airplane

The airplane used in the tests was a conventional propeller-driven, low-midwing, single-place, fighter airplane. A three-view drawing and a photograph of the airplane as instrumented for flight tests are given in figures 1 and 2, respectively.

Dihedral-Effect Control Apparatus

Theory and design conditions.- Dihedral effect can be expressed quantitatively by the stability coefficient C_{l_β}, the rate of change of rolling-moment coefficient with angle of sideslip. The design of the present apparatus is based on the fact that a change in apparent C_{l_β} can be obtained from actuation, by a servo mechanism with an output motion δ proportional to sideslip angle β, of a control surface which produces rolling moment. Then

$$\left(\Delta C_{l_\beta}\right)_s = C_{l_\delta}\left(\frac{\partial \delta}{\partial \beta}\right)_s \qquad (1)$$

where

$\left(\Delta C_{l_\beta}\right)_s$ change in C_{l_β} due to servo action

C_{l_δ} rolling effectiveness of surface controlled by servo

$(\partial\delta/\partial\beta)_s$ servo gearing

Preliminary investigation showed that the most practicable method of obtaining large servo-actuated rolling-moment coefficients proportional to sideslip angle on the test airplane was by use of the normal ailerons. In order to simulate changes in C_{l_β}, the servo motion of the ailerons must not be accompanied by any resultant movement of the stick or increment in lateral stick force. This condition arises from the fact that the aileron stick-deflection and stick-force gradients $d\theta/d\beta$ and $dF/d\beta$ required for balance in steady straight sideslips are, to a pilot, measures of the stick-fixed and stick-free dihedral effect. In order to obtain changes in $d\theta/d\beta$ and apparent stick-fixed C_{l_β}, a differential linkage is required in the control system, with aileron deflection as the output

and pilot-applied stick motion and an independent servo motion as inputs. The maximum value of servo-gear ratio $(\partial\delta_a/\partial\beta)_s$ which then can be utilized is restricted in two ways: First, the maximum servo-actuated aileron deflection must be limited to allow the pilot sufficient aileron deflection for normal maneuvering and emergency control; and, second, the minimum sideslip-angle range over which the apparatus is operative for any servo-gear ratio must be greater than that required for normal operation and the desired test maneuvers. These restrictions become more severe as airspeed is decreased, since both the pilot-required aileron control and the sideslip-angle range then generally increase.

In order to obtain changes in $dF/d\beta$ and apparent stick-free C_{l_β}, a means of canceling out the hinge moment due to servo-actuated deflection of the ailerons is required, since with common differential linkages the entire hinge moment is transmitted back to the stick. It was desired for the first tests that the ratio of the stick-free value of C_{l_β} to the stick-fixed value remain constant as the stick-fixed value was changed. This leads to the requirement that the stick-free value be zero when the stick-fixed value is zero, which is equivalent to assuming that the change in aileron hinge moment with sideslip is zero. The desired effect is approximated on the present installation by servo actuation of the aileron trim tab to furnish an aileron hinge moment equal and opposite to that arising from the servo-actuated aileron motion. As was the case for the aileron system, a differential gearing with tab angle as the output motion and the tab servo and pilot-actuated trim-tab motions as inputs is required.

Although the discussion thus far has been confined to the static flight condition of steady straight sideslips, a similar explanation which yields similar requirements can be developed for maneuvers in which sideslip angle varies rapidly. The ideal servo mechanism for producing a change in C_{l_β} which is constant under any dynamic condition would be one with an output motion always in phase with and a constant proportion of the input quantity. Deviations of actual servo mechanisms from this ideal cause undesired variations in C_{l_β}.

Aileron drive system.- There are a number of mechanisms which will give the desired differential aileron motion, and the choice between them depends on the particular control system under consideration. The linkage which was used for the test airplane is illustrated schematically in figure 3. In the original aileron circuit, lateral stick motion imparted a corresponding angular motion to a control horn attached to the forward end of a torque tube which was

supported by two fixed bearings. This rotation was transmitted as a linear motion by push rods attached by self-alining bearings to the horn. In the modified installation an additional torque-tube bearing was attached to the fuselage structure just forward of the stick. The torque tube was cut immediately forward of this bearing and a universal joint installed. The original forward fixed bearing was replaced by two bearings free to move in a horizontal plane. The one nearest the torque-tube horn restrains the tube vertically by means of roller guides. The other is bolted to a plate which has a pin joint centered over the universal joint. This plate is attached by cables to a drum on the servo motor and rotates in a horizontal plane when the drum rotates. Thus, the forward portion of the torque tube swings about the universal joint when the servo responds to a sideslip signal. The torque-tube horn and the aileron push rods then move laterally if the stick is held fixed, and this motion results in an aileron deflection proportional to drum rotation. The pilot still can apply in the normal manner any additional desired aileron deflection up to maximum in either direction. The kinematics of the revised system are shown in figure 4, in which total aileron deflection δ_a (the sum of left and right aileron angles) is plotted as a function of lateral stick deflection θ for neutral and maximum test servo positions. These curves and additional data obtained at intermediate servo positions showed that, as is desired, the gearings $\partial\delta_a/\partial\theta$ and $(\partial\delta_a/\partial\beta)_s$ are nearly constant over the available ranges of δ_a and θ.

Aileron servo mechanism.- The aileron and tab servo mechanisms were developed from an electric amplidyne system normally used for remote control of aircraft gun turrets. This system was chosen on the basis of signal-system and motor-output requirements, applicability to aircraft, and availability. A simplified electrical circuit diagram of the installation is given in figure 5. The error-measuring portion of the aileron servo mechanism is essentially a two-potentiometer bridge circuit with a 30-volt, 400-cycle power supply. One potentiometer is geared mechanically to a yaw vane located on a boom extending forward from the left wing tip of the airplane. The second potentiometer is connected to the aileron servo motor. With the yaw vane and servo motor initially neutral, the bridge circuit is at one balance point. When the vane is deflected through an angle of sideslip β, an error signal is supplied by the bridge to the amplifier. The amplified signal, converted to direct current, is fed to the field of an amplidyne generator the armature of which is driven continuously at constant speed by the d-c. amplidyne motor. The generator output voltage, of

a polarity and magnitude determined by the error signal, is applied to the armature of the reversible separately excited d-c. aileron servo motor. The generator output voltage determines the direction and speed of the servo-motor rotation, which moves the torque tube and attached potentiometer in the direction which tends to balance the bridge circuit at a new point corresponding to β and $(\delta_a)_s$. The servo gearing $(\partial\delta_a/\partial\beta)_s$ can be altered through the switch S_1, which in effect varies the bridge unbalance voltage per degree sideslip. The sign of $(\partial\delta_a/\partial\beta)_s$, and thus $(\Delta C_{l_\beta})_s$, can be reversed by switch S_2.

Aileron tab drive and servo mechanism.- The ratio $(d\delta_t/d\delta_a)_s$ of the tab motion to aileron motion required to balance the hinge moment due to servo-actuated aileron motion was determined from preliminary flight tests. Insufficient total power of the original trim tab necessitated an increase of both the area and the control throw of the tab, which was located on the left aileron. (See fig. 6.) Brief flight tests with this revised tab yielded a $(d\delta_t/d\delta_a)_s$ value of -1.15, which was used for the present tests. Although the standard aileron trim-tab drive linkages passed near the aileron servo-motor location in the cockpit, it was not possible to utilize this servo motor in obtaining the desired tab action $(d\delta_t/d\delta_a)_s$ because of excessive lost motion in the tab linkages between cockpit and tab surface. Therefore, a separate servo motor was installed in the left wing to drive the tab more directly. (See fig. 6.) As indicated by figure 5, the tab servo-electrical circuit is similar to the aileron circuit, although selsyns are used in place of potentiometers in the signal network. Error signals arising from rotation of the selsyn attached to the aileron servo result in motions of the tab servo and selsyn which tend to reduce the error to zero. The ratio $(d\delta_t/d\delta_a)_s$ is the constant value of -1.15. The pilot is furnished with a trim-tab control which, when rotated, acts through differential gearing to rotate the aileron motor selsyn and, hence, the aileron tab.

Servo-mechanism controls and operating procedure.- The location of the aileron drive system and associated cockpit controls is shown in figure 7; the main servo-control box is shown in more detail in figure 8. When the apparatus is operated in flight, the error-signal circuits are energized first. The desired value of $(\partial\delta_a/\partial\beta)_s$ then is set with the servo-gearing ratio-selector switch, which gives values ranging from maximum positive to maximum negative in six approximately equal increments. Ammeters, which indicate the aileron servo-error signal, reduce the possibility of abrupt motions

which might occur if the servo motor were energized with the airplane at a sizable angle of sideslip. The pilot, by use of the rudder, reduces the error signal to zero and then places the entire system in operation by switching on the aileron amplidyne. Changes in C_{l_β} then are easily obtainable at any time by reducing the sideslip angle to zero and moving the servo-gearing selector switch. Both the aileron and the tab drives are equipped with limit switches and with locking and emergency drive circuits which permit the pilot to lock or return to neutral the torque tube and tab in the event of malfunctioning.

Instrumentation

Standard NACA photographically recording instruments were used to measure as a function of time the following variables: indicated airspeed; pressure altitude; applied aileron control force; angular positions of the aileron surfaces, aileron tab, aileron servo drum, forward portion of the aileron torque tube in the horizontal plane, rudder, and stick; sideslip angle; and airplane rolling and yawing velocities. A free-swivelling pitot-static head mounted on a boom extending forward from the right wing tip was used for airspeed and altitude measurements. The recording sideslip vane was mounted on a parallel boom at the same planwise location relative to the wing as the servo-error-signal vane on the left wing tip. (See fig. 2.) Comparison of simultaneous records obtained in flight from vanes on these two booms showed a difference in indicated sideslip angle which was small and constant within about $\pm 0.2^\circ$ over the test airspeed and sideslip-angle range.

TESTS AND RESULTS

The results presented in this report are based on data obtained during the first flights of the test airplane made with the complete dihedral-effect control apparatus in operation. The primary purpose of these early tests was to determine, from recorded data and pilots' opinions, the ability of the apparatus to simulate changes in stick-fixed and stick-free dihedral effect under static and dynamic flight conditions. Although data were obtained at several airspeeds and values of servo gearing $(\partial\delta_a/\partial\beta)_s$, results presented herein are confined to the normal airplane (servo inoperative) and to the maximum test values of $(\partial\delta_a/\partial\beta)_s$ or $(\Delta C_{l_\beta})_s$ at a nominal indicated airspeed of 350 miles per hour. The data presented are typical, and

these test conditions approximate those originally considered in the design of the apparatus. Operation under static flight conditions was studied in steady straight sideslips and under dynamic conditions in abrupt rudder kicks and cockpit-control-fixed lateral oscillations.

Steady straight sideslips.- The aileron and tab deflections supplied by servo action and the net balancing aileron deflection and stick force supplied by the pilot are plotted in figure 9 as a function of sideslip angle for the three test servo-gearing ratios. All quantities represent changes from the wings-level trim condition. Corrections for distortion in the aileron servo drive system (between the aileron servo motor and the torque tube) have been made.

The following formula was used in computing the values of stick-fixed C_{l_β} noted in figure 9:

$$C_{l_\beta} = C_{l_p}\left[\frac{d(pb/2V)}{d\delta_a}\right]\left(\frac{\partial\delta_a}{\partial\beta}\right) \tag{2}$$

where a C_{l_p} value of -0.45 was obtained from reference 2. Abrupt rudder-fixed aileron-roll flight tests gave a value of -0.00215 for $d(pb/2V)/d\delta_a$ (corrected approximately for effects of sideslip), and $\partial\delta_a/\partial\beta$ is the pilot-applied curve slope from figure 9. Also shown for comparison are values of the stick-fixed effective dihedral angle Γ_e computed from the equation

$$\Gamma_e = \frac{C_{l_\beta}}{C_{l_\beta}/\Gamma} \tag{3}$$

where a value of C_{l_β}/Γ of -0.000225 per degree squared was obtained from reference 2.

Abrupt rudder kicks.- The pilot abruptly deflected and held the rudder pedals while the stick was held fixed. Several different rudder deflections, left and right, were employed for each servo-gearing ratio. Typical time histories showing the motions of the control surfaces and airplane are presented in figure 10. The computed aileron deflections due to servo action for an ideal servo mechanism (no time lag) are shown for comparison with the measured values. The variation of the maximum value of the rolling parameter $pb/2V$ with change in rudder deflection $\Delta\delta_r$ for these maneuvers is given in figure 11(a). The ratio of $pb/2V$ per unit $\Delta\delta_r$ for each servo-gearing ratio to the value for the normal airplane $[(\partial\delta_a/\partial\beta)_s=0]$ was computed from the slopes of these curves and is shown in

figure 11(b) as a function of the corresponding static stick-fixed effective dihedral angle. A similar predicted curve computed by the method of reference 3 is shown for comparison.

Control-fixed lateral oscillations.- Lateral oscillations were induced from an initial steady-sideslip attitude by abruptly returning and holding the rudder pedals and control stick in trim position. Typical time histories of the control deflections, including the computed aileron motion supplied by an ideal servo mechanism, and resultant airplane motions are given in figure 12. The absolute values of servo-applied aileron deflection shown in figure 12 are probably in error because of initial misalinement at the trim sideslip angle. This factor is not important, however, because it is only the time variation of this quantity that has any significance here. The computations of aileron deflection which would be supplied by an ideal servo were based on exact agreement in the steady sideslip. The oscillation period P and number of cycles to damp to one-half amplitude $C_{\frac{1}{2}}$ were determined from the time histories of sideslip angle, and are plotted in figure 13 as a function of Γ_e. Values of P and $C_{\frac{1}{2}}$ computed by the method of reference 4 are also shown. In general, the best available data on the mass and aerodynamic characteristics were employed in the computations, but minor adjustments were made to give exact correlation for the normal airplane in order to facilitate comparison of the measured and predicted effects of C_{l_β}

DISCUSSION

Characteristics of Effective-Dihedral Control in Steady Sideslips

During steady sideslips, the pilot noted that the apparatus did not cause the airplane to have an artificial feel; that is, it caused no significant difference in the feel of the airplane from that which would be expected of an airplane with actual dihedral of the magnitudes being simulated by the apparatus. Figure 9 shows desirable smooth and linear variations of pilot-applied aileron deflection and stick force with sideslip angle with the apparatus in operation. The slope of the pilot-applied aileron-deflection curve varies, for the maximum test aileron servo-gear ratios, from a large stable value to a noticeably unstable value, corresponding to a stick-fixed C_{l_β} range from -0.0033 to 0.0006 and a Γ_e range from 14.9°

to -2.7°. Since the normal value of Γ_e is 6.3°, the servo action caused about $\pm 9^\circ$ change. The slope of the stick-force curve varies from a large stable value to approximately zero, indicating large changes in stick-free dihedral effect. However, the force-curve slope is zero when the aileron-deflection-curve slope is unstable; thus, the desired condition that the stick-free C_{l_β} and the stick-fixed C_{l_β} equal zero at the same gearing ratio was not accomplished for these tests. This condition could be rectified by increasing the tab servo-gearing ratio $(d\delta_t/d\delta_a)_s$ or the tab effectiveness. The latter solution appears preferable in the present application because of possible loss in effectiveness of the tab at the large deflections which would result from increases in $(d\delta_t/d\delta_a)_s$.

The sizable Γ_e range from 14.9° to -2.7°, which was obtained in the present tests, corresponds closely to that originally desired for the investigation of the high-speed dynamic lateral characteristics with the test airplane. It is believed that, as more data and experience are gained with the apparatus, the aileron servo-gearing ratio can be increased gradually to give about twice the present $\Delta\Gamma_e$ of $\pm 9^\circ$, so that the characteristics of configurations such as highly swept-back and triangular wings can be more closely simulated.

Characteristics in Abrupt Rudder Kicks

The response in roll to a given abrupt rudder deflection is one measure of dihedral effect. The rolling-velocity curves of figure 10 show that, qualitatively, the apparatus successfully simulated large changes in dihedral effect under these severe dynamic conditions; the changes in maximum rolling velocity with servo-gearing ratio (and static Γ_e) are readily apparent. It is seen that the actual servo-applied aileron deflection is in good agreement with the values computed from the sideslip angle for an ideal servo, except for a time lag of about 0.1 second during the initial portion of the maneuver. The records and computations showed that this time lag did not have a serious effect on the rolling response in simulating positive changes in Γ_e (fig. 10(b)), but that it caused an undesired initial rolling response when attempting to simulate large negative changes in Γ_e. With the apparatus set for $\Gamma_e = -2.7^\circ$, the measured response to left rudder deflection showed an initial small left rolling velocity prior to the development of right rolling velocity (fig. 10(c)). The computed response showed right rolling velocity throughout the maneuver. There was good agreement, however, between the values of computed and measured maximum rolling velocities and the times at which they occurred. Additional step-by-step response

calculations were made, and the results showed that a lag of 0.1 second would account for the undesired initial left roll. Close examination of position-recorder data showed that the lag in servo-applied aileron deflection was due partially to lag in the servo-mechanism response and partially to stretch in the servo-control system between the servo motor and the torque tube. Suitable minor adjustments in the electrical circuit might improve the servo response in future tests. Reduction of the lag due to stretch could be accomplished by a reduction in the flexibility and inertia of the control system, but this would necessitate major changes in the present apparatus.

The effect of this small amount of lag was noticeable to the pilots, but, in their opinion, it did not cause the airplane to have an artificial feel. To the pilots, the small amount of reverse rolling velocity appeared as an effect of yawing velocity, and their opinion was that the apparatus satisfactorily simulated changes in dihedral.

A quantitative measure of the effect of the apparatus in changing the rolling response in abrupt rudder kicks is given by figure 11. The small initial undesired rolling motion at the -2.7° Γ_e setting was ignored in deriving these data. It is seen from figure 11(a) that the maximum value of the rolling parameter $pb/2V$ per unit rudder deflection, a measure of dihedral effect, was varied over the wide range from the normal value of 0.005 to 0.011 and -0.002. Figure 11(b) shows good agreement between the measured and predicted effects of Γ_e on the rolling response, and thus indicates that the effects of the desired changes in Γ_e are simulated by the apparatus under severe dynamic conditions.

It is believed that the initial small adverse rolling motion experienced in rudder kicks when the apparatus was used to simulate the -2.7° value of Γ_e will not prove a serious deficiency in applying the apparatus to further dynamic-stability studies. This effect would be most noticeable when attempting to simulate smaller negative (or zero) dihedral effect. As more negative values of Γ_e are obtained by increasing the servo gearing, the initial left rolling velocity following a left rudder kick should decrease slightly and the ultimate right rolling velocity will increase, possibly to the point where the undesired initial motion will not be noticeable to the pilot. The rudder kick is a severe maneuver, of use primarily in flight testing; the desirability of coordinated maneuvers and the large time lag between application of rudder deflection and attainment of substantial rolling velocity precludes its use in normal flying. The magnitude and rate of change with time of

sideslip angle (and the resultant servo lag) attained in this maneuver are much greater than usually experienced in maneuvers at high speed. The only sideslip-angle changes of comparable abruptness which might occur in the proposed dynamic-stability investigation would be those in very gusty air.

Characteristics in Lateral Oscillations

As was the case for the rudder kicks, the servo-applied aileron deflection lags the sideslip angle a small amount in the lateral-oscillation time histories shown in figures 12(b) and 12(c). There are occasional small irregularities in the servo-output motion, but the agreement between actual and ideal aileron deflection is considered good. The time histories show that, qualitatively, the apparatus simulates the effects of changes of C_{l_β} on lateral-oscillation characteristics. Compared to the normal characteristics (fig. 12(a)), the increased excitation of the rolling motion and the decreased damping of the airplane motions caused by an increase in dihedral effect (fig. 12(b)) are apparent. With a slight negative dihedral effect (fig. 12(c)), the rolling motion is small, and the airplane motions are rapidly damped.

Fair quantitative agreement between measured and predicted oscillation period and damping are shown in figure 13. The discrepancies at the -2.7° static effective-dihedral-angle setting may be due in part to difficulties in accurately evaluating the oscillation flight data when, as in this case, the damping is high, and due in part to the slight rudder motions which the pilot was unable to eliminate. Both the measured and predicted effects of Γ_e on the period are small. The measured decrease in damping with increasing Γ_e is approximately the same as that given by the predictions, which shows that deviations of the aileron servo characteristics from the ideal did not have a serious effect on the airplane damping.

It is believed that, with suitable minor modifications, the apparatus will be capable of producing sufficiently large positive dihedral effect to cause oscillatory instability.

CONCLUDING REMARKS

The first flight tests of a new apparatus for varying the dihedral effect of a conventional fighter-type airplane have shown that the device permits large changes in stick-fixed and stick-free

dihedral effect to be made readily in flight. Successful tests have been conducted over an effective-dihedral-angle range from 14.9° to -2.7°.

The apparatus exhibited a small amount of lag during dynamic maneuvers which, although perceptible to the pilots, was not considered by them to cause any significant change in the feel of the airplane from that of an ordinary airplane with similar dihedral.

Extension of the operating ranges of the dihedral apparatus is now being made over a limited angle of sideslip range, so that the large change of dihedral effect with lift coefficient experienced on swept-back wings can be simulated. Determination of the tolerable limits in both the negative and positive direction is of special interest.

Ames Aeronautical Laboratory,
National Advisory Committee for Aeronautics,
Moffett Field, Calif.

REFERENCES

1. Morgan, M. B.: Control in Low-Speed Flight. Aeroplane, vol. 73, Sept. 5, 1947, pp. 281-283.

2. Pearson, Henry A., and Jones, Robert T.: Theoretical Stability and Control Characteristics of Wings with Various Amounts of Taper and Twist. NACA Rep. No. 635, 1938.

3. Harper, Charles W., and Jones, Arthur L.: A Comparison of the Lateral Motions Calculated for Tailless and Conventional Airplanes. NACA TN No. 1154, 1947.

4. Sternfield, Leonard: Effect of Product of Inertia on Lateral Stability. NACA TN No. 1193, 1947.

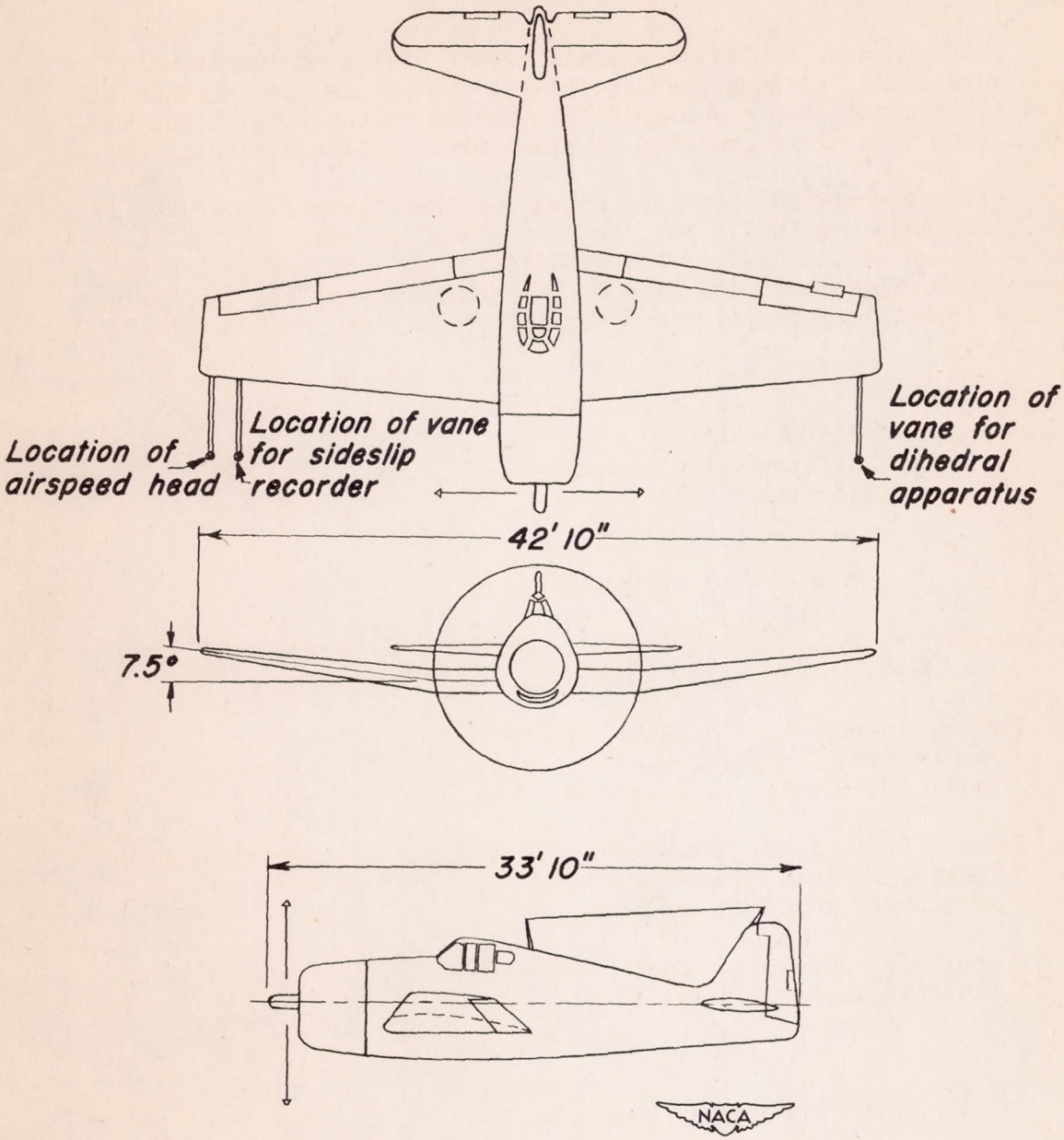

Figure 1.- Three-view drawing of the test airplane.

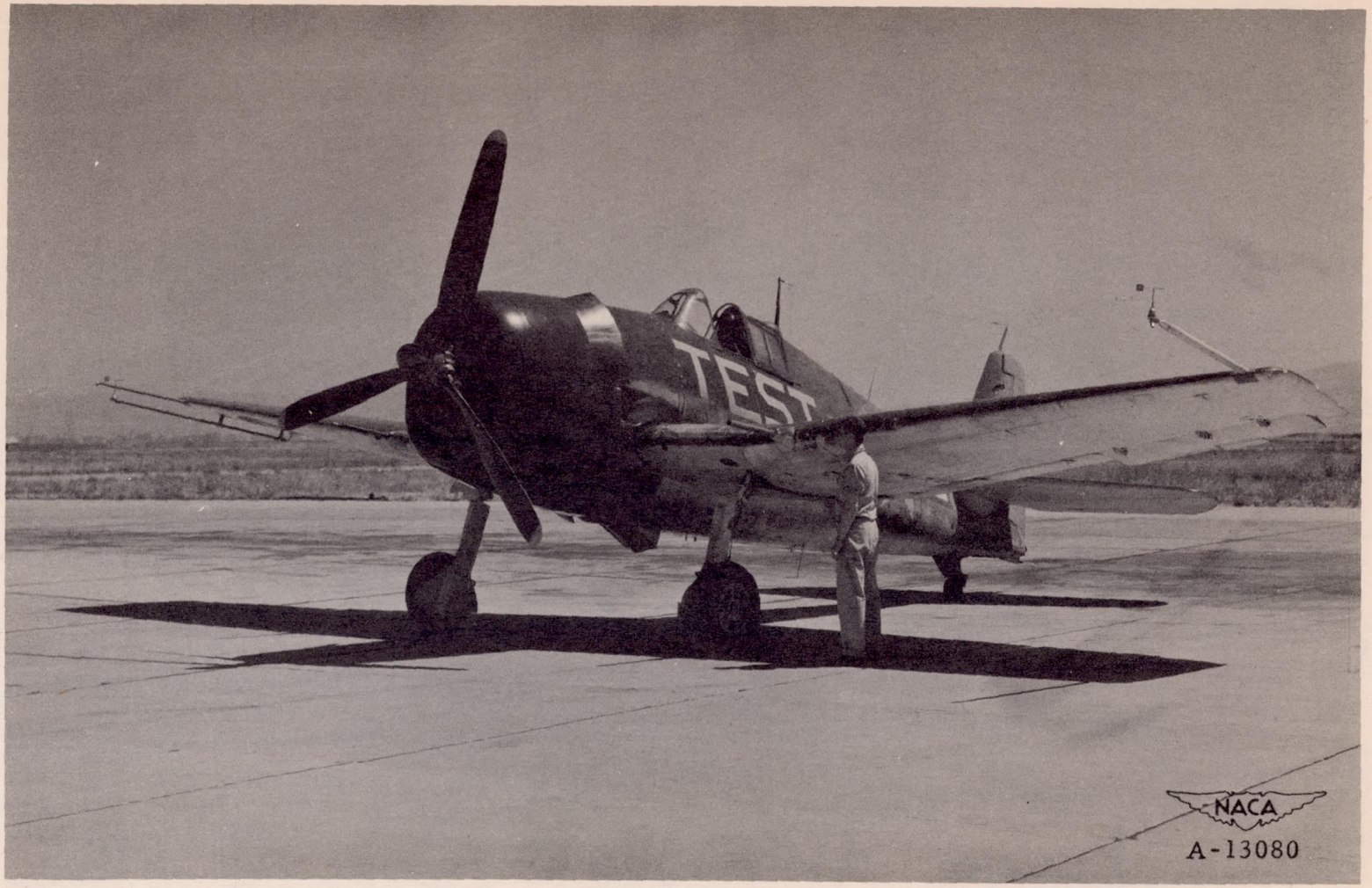

Figure 2.- Three-quarter front view of the airplane as instrumented for flight tests.

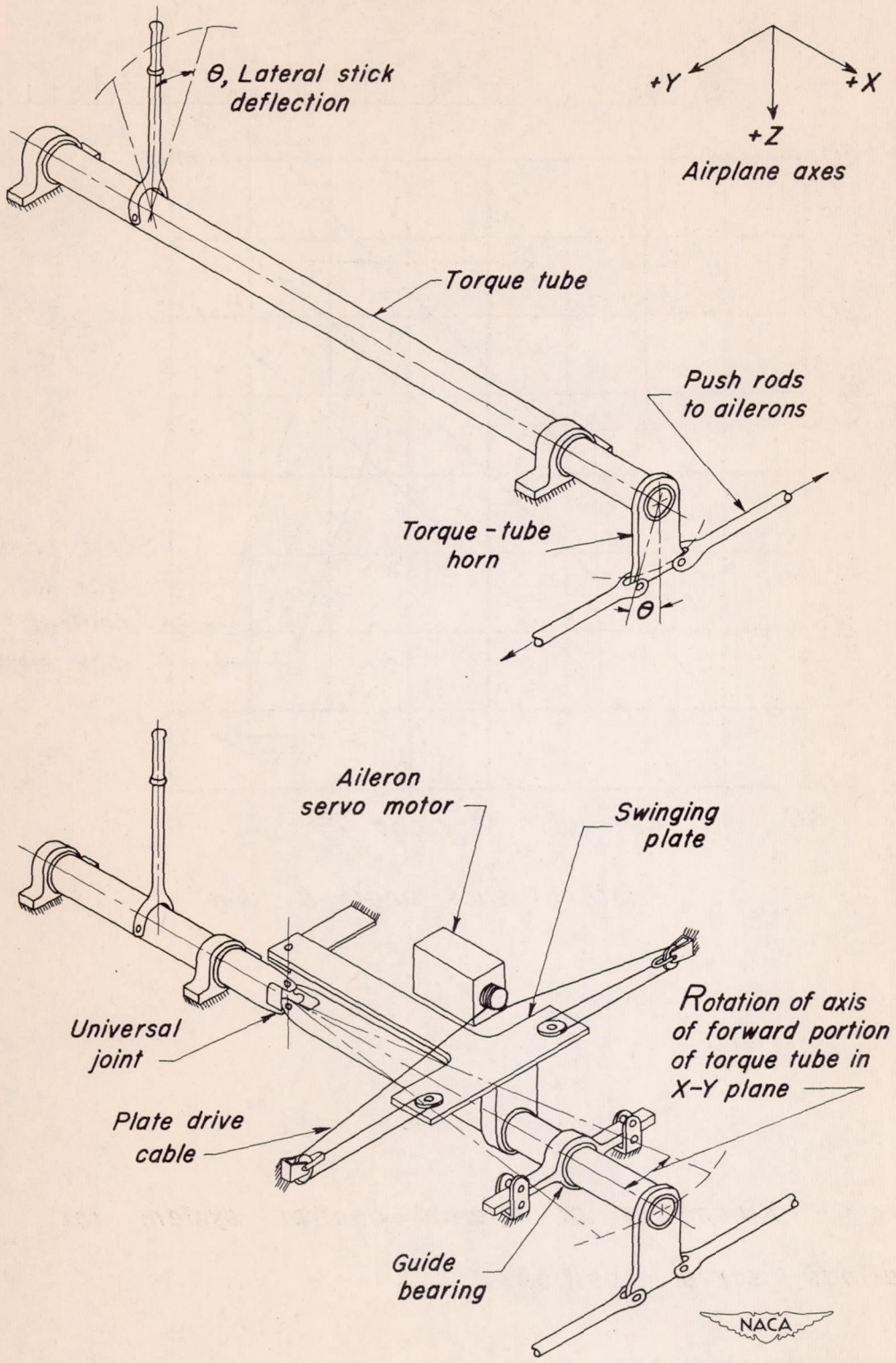

Figure 3.- Sketch of original and modified aileron control system.

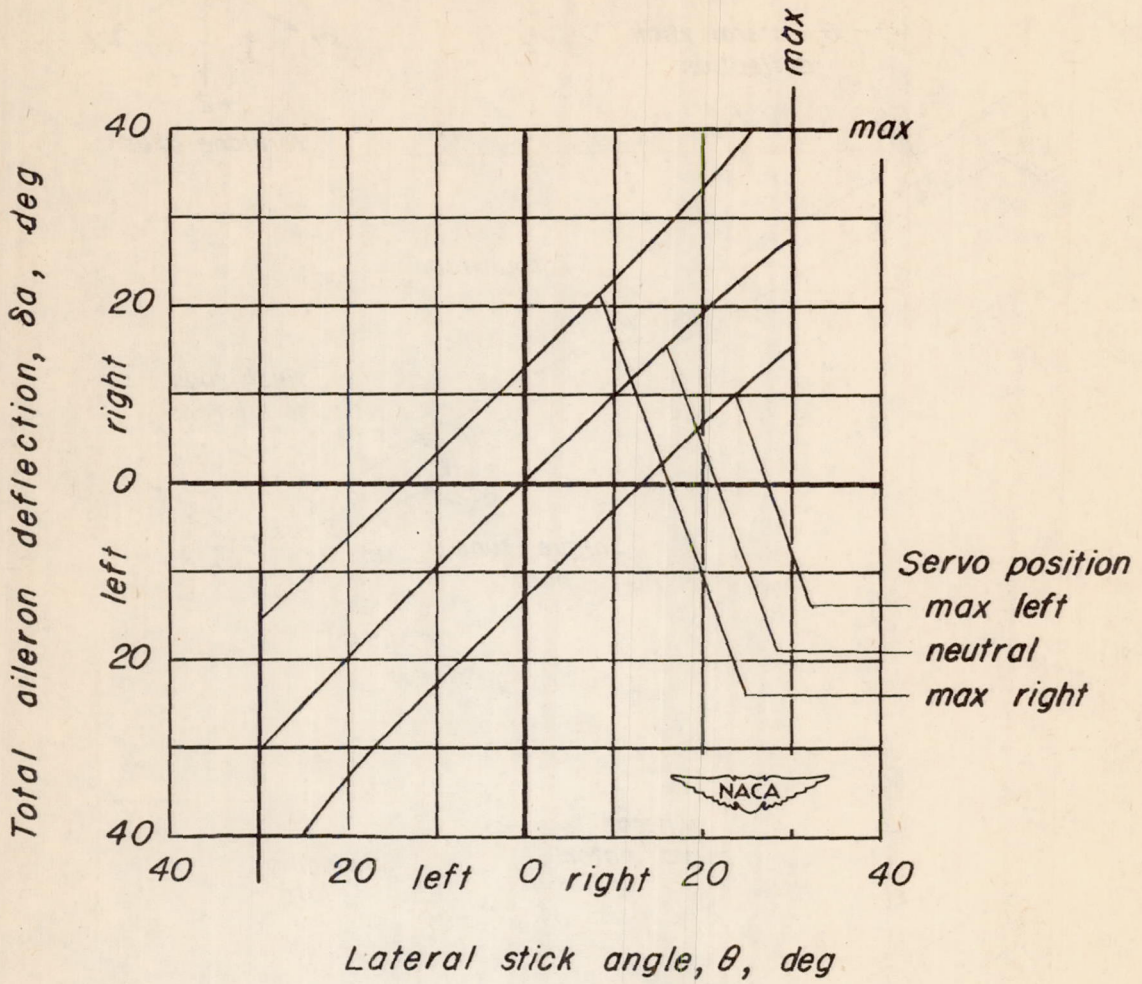

Figure 4.– Kinematics of aileron control system for various servo positions.

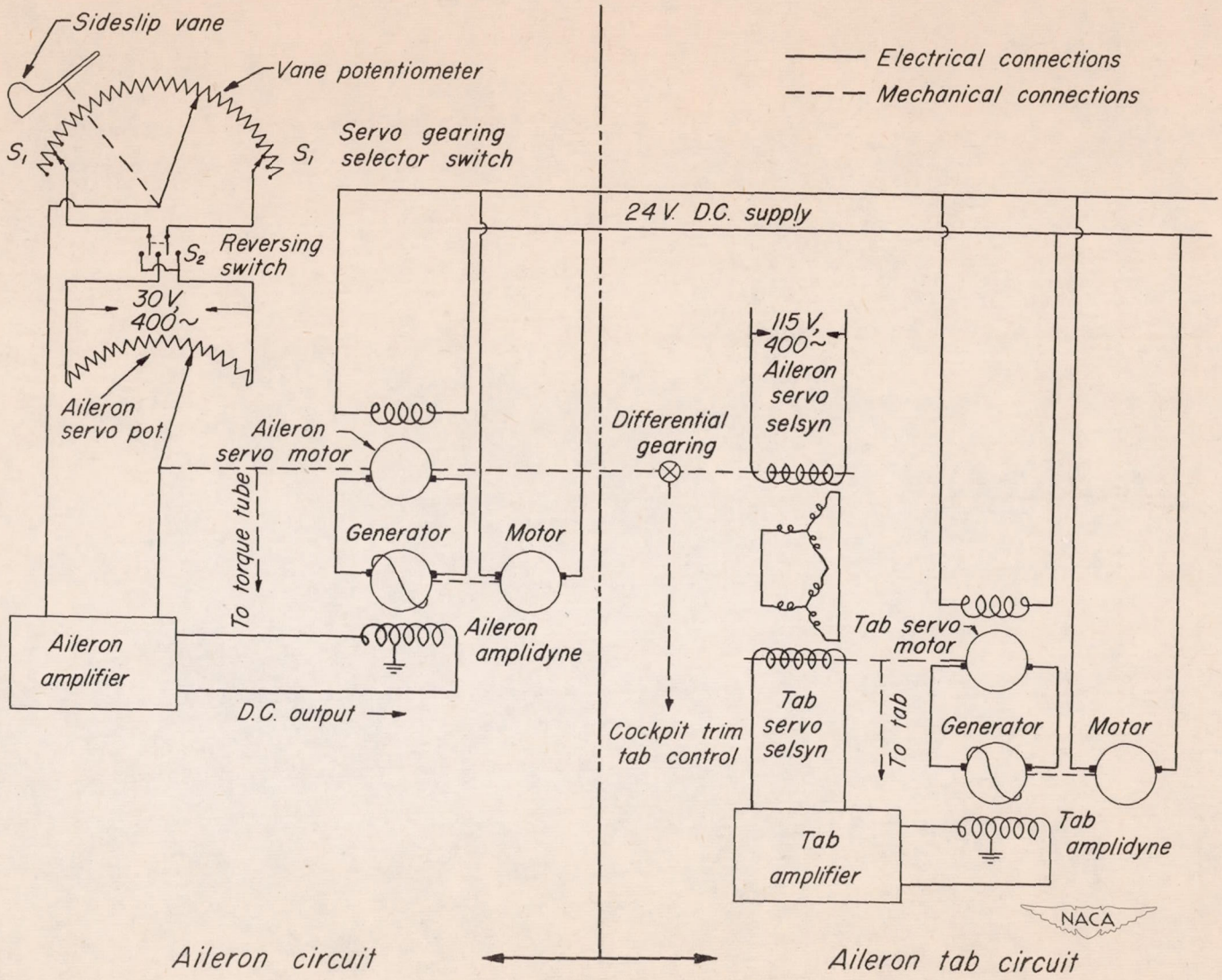

Figure 5.- Simplified electrical circut diagram of the dihedral-effect control apparatus.

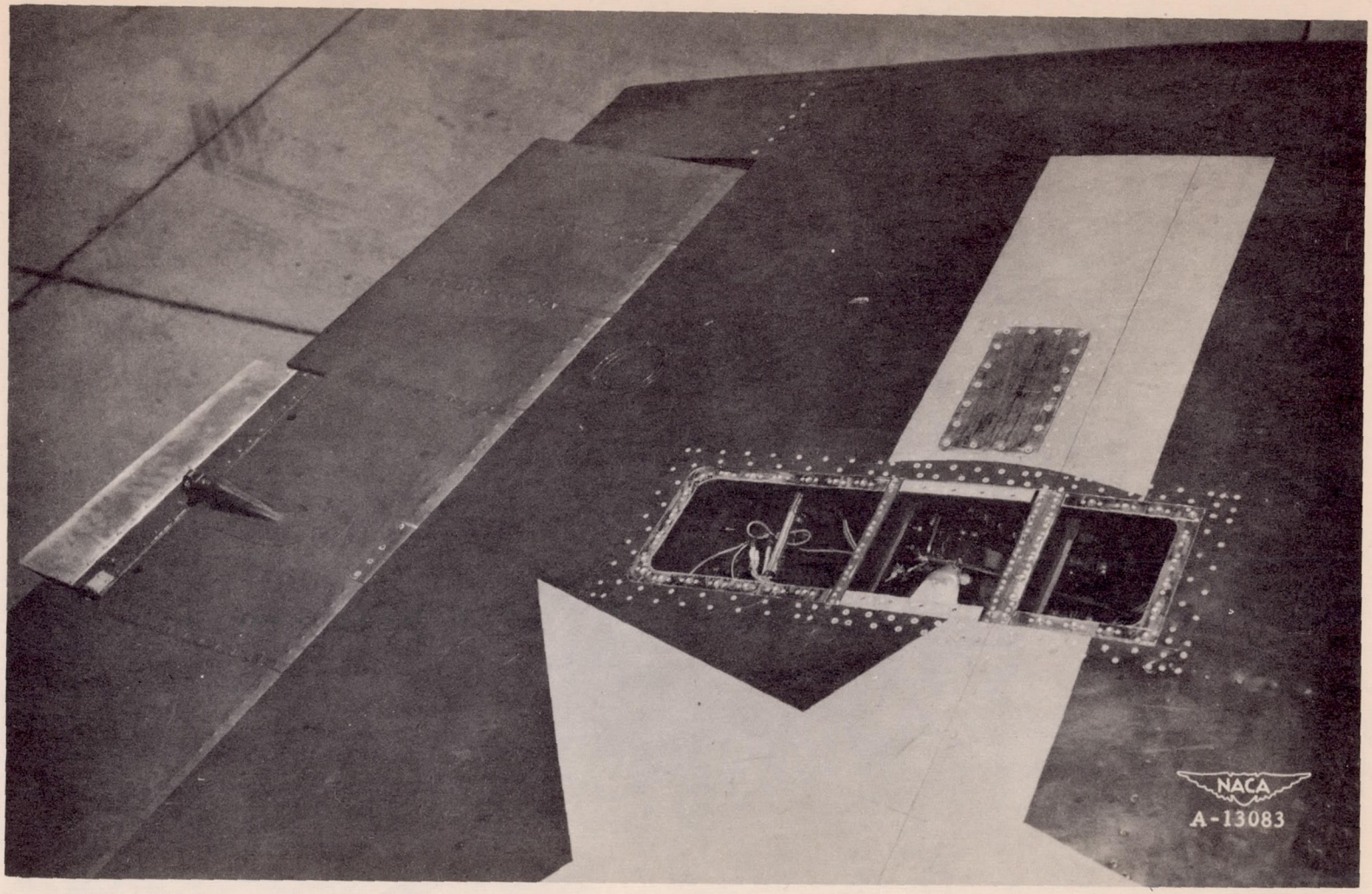

Figure 6.– Top view of left outer wing panel, showing modified aileron tab and tab servo–drive unit location.

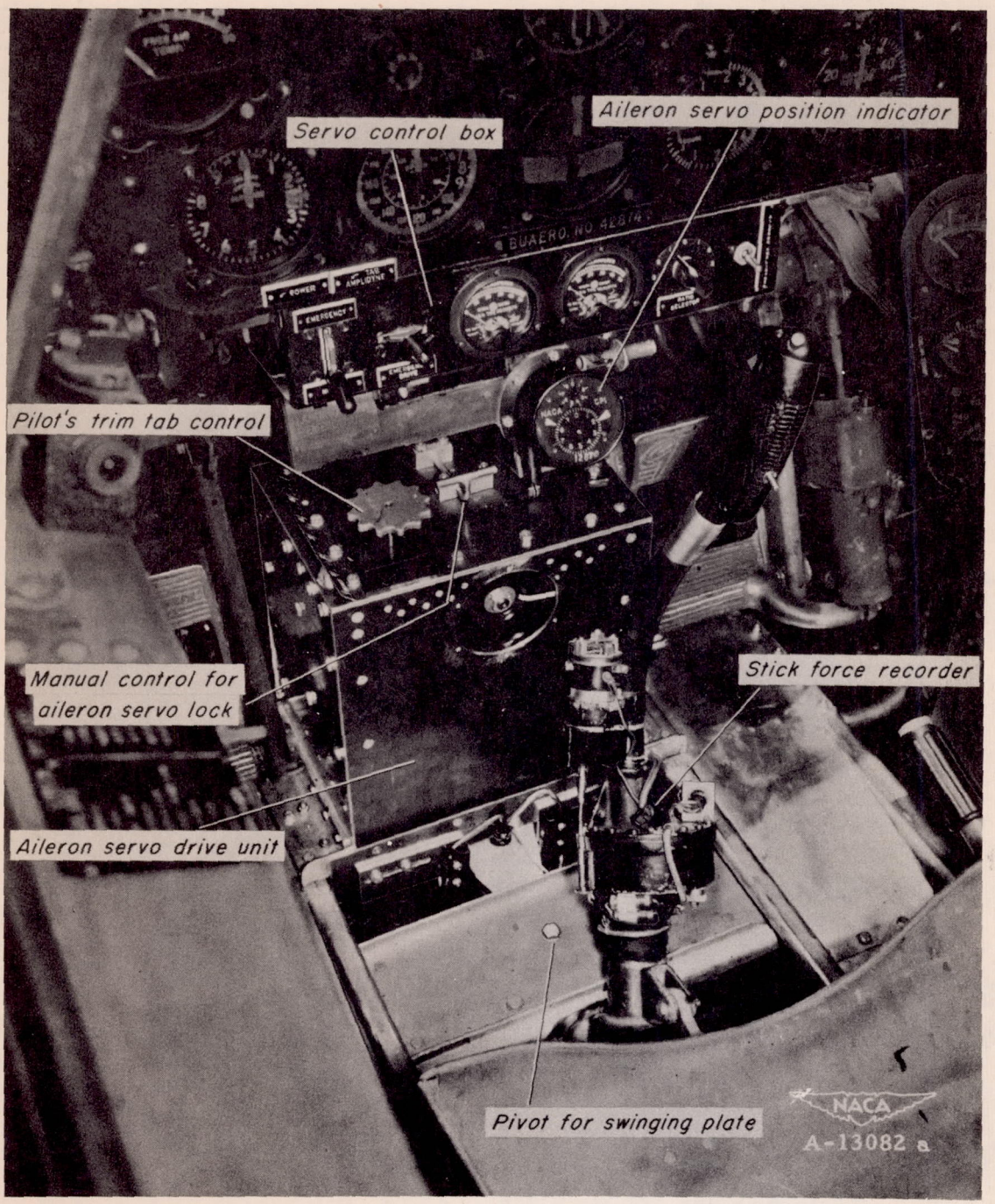

Figure 7.– View of cockpit interior showing aileron servo–drive and control components.

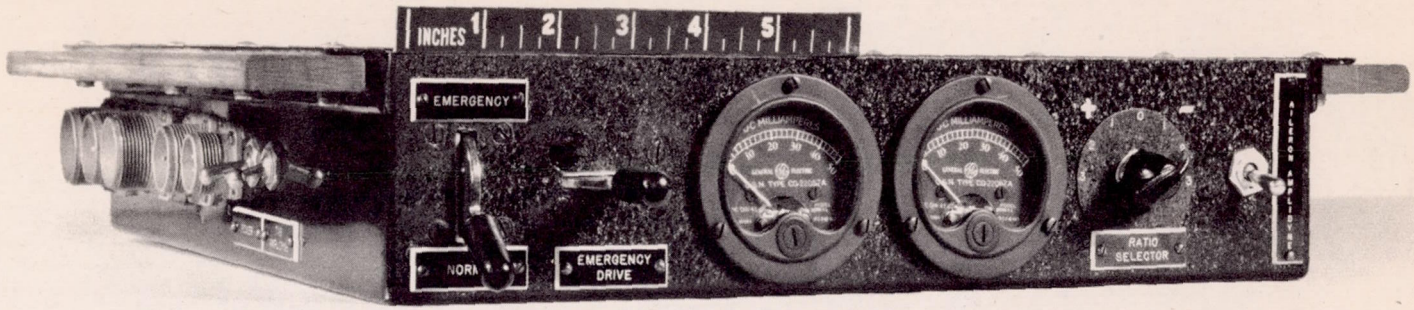

NACA
A-13172

Figure 8.- Three-quarter front view of control box for the dihedral-control apparatus.

NACA
A-13175

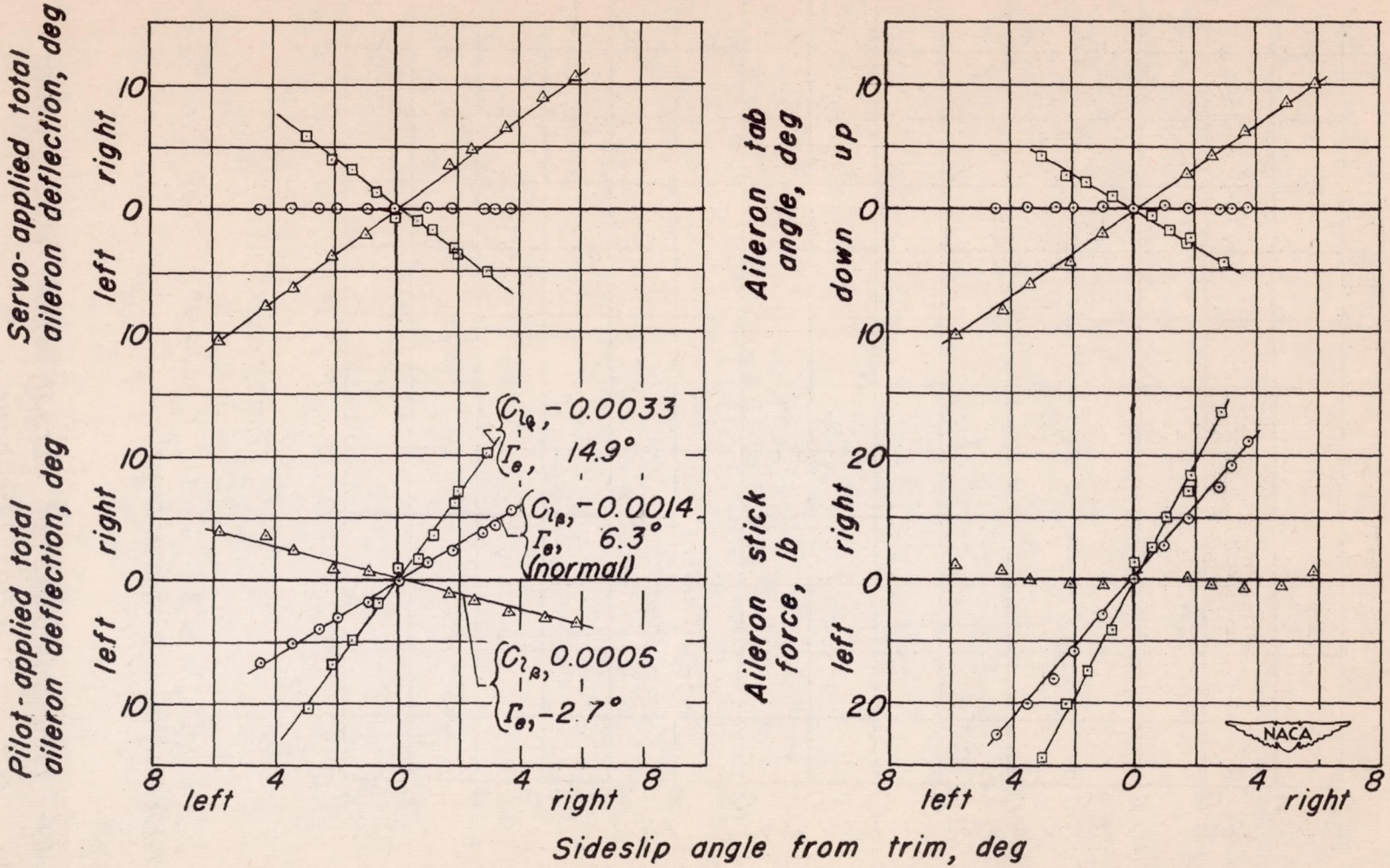

Figure 9.- Lateral control characteristics in steady straight sideslips. V_i = 350 miles per hour.

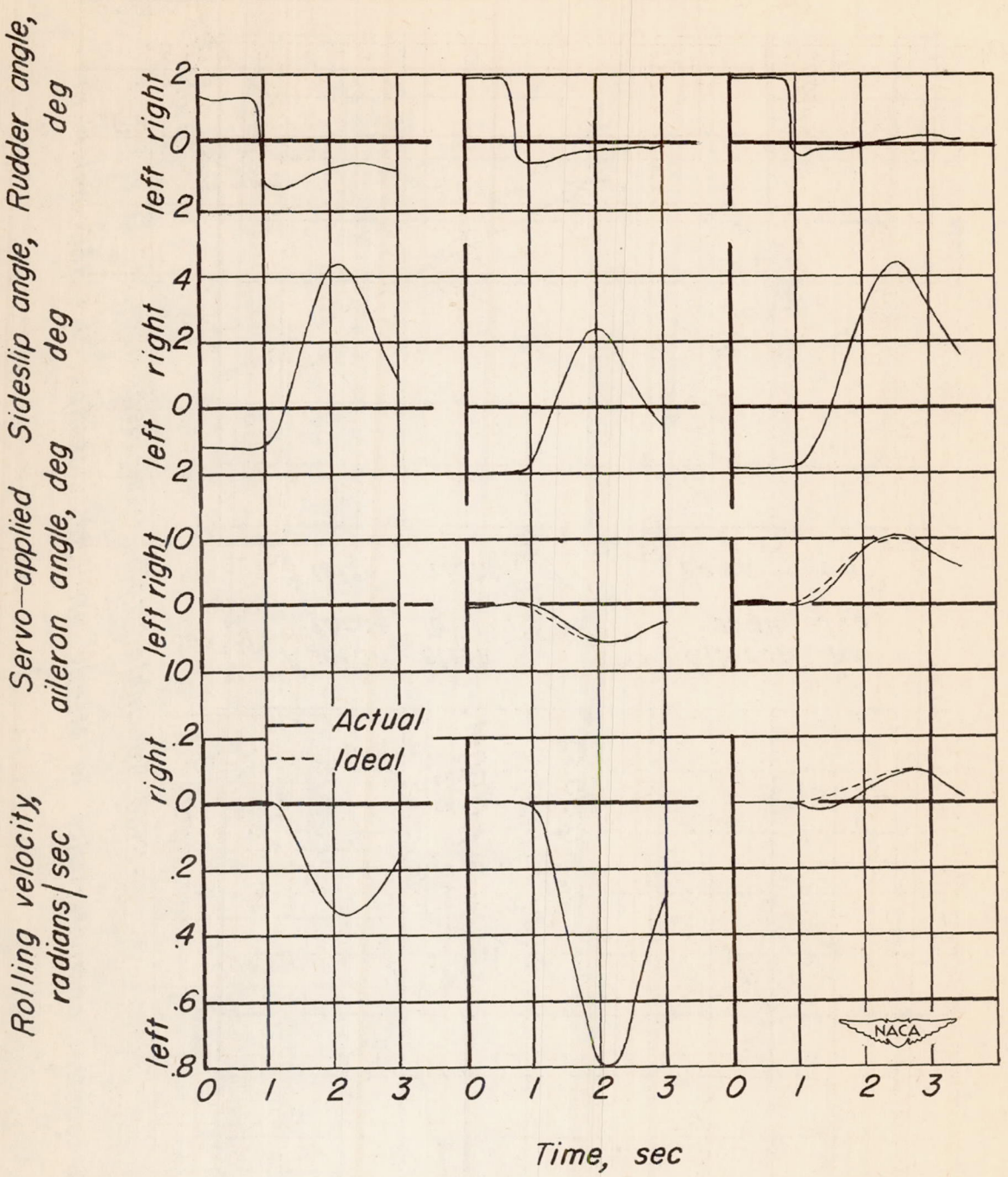

(a) $\Gamma_e = 6.3°$ (b) $\Gamma_e = 14.9°$. (c) $\Gamma_e = -2.7°$. (normal, servo inoperative).

Figure 10.- Time histories of abrupt, stick-fixed rudder kicks. V_i = 350 miles per hour.

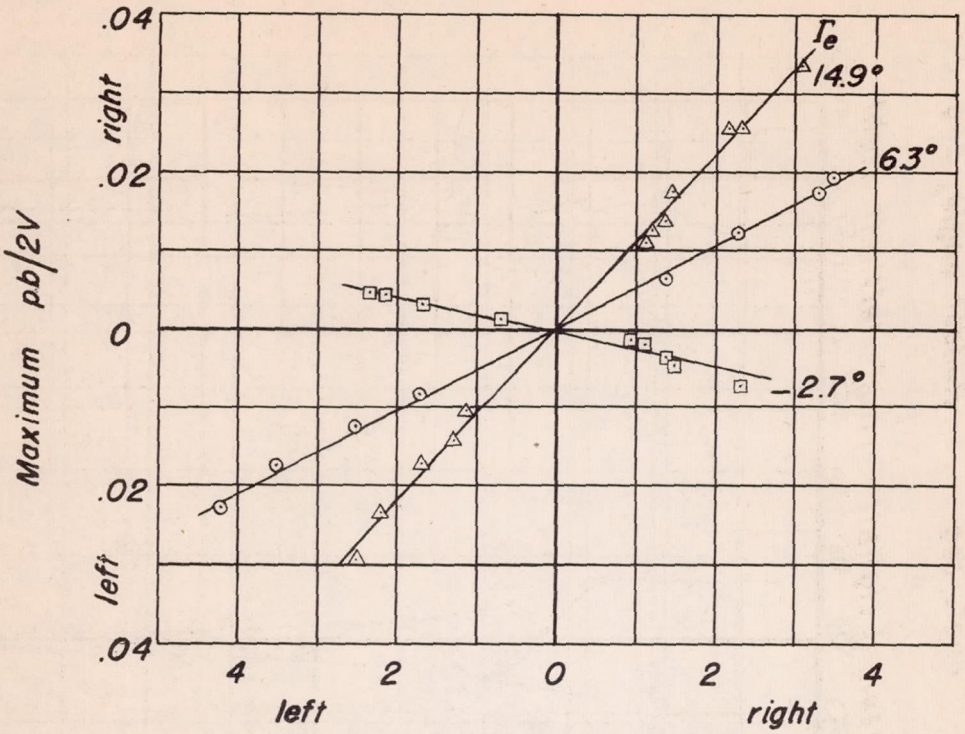

(a) Variation of maximum pb/2V with $\Delta\delta_r$.

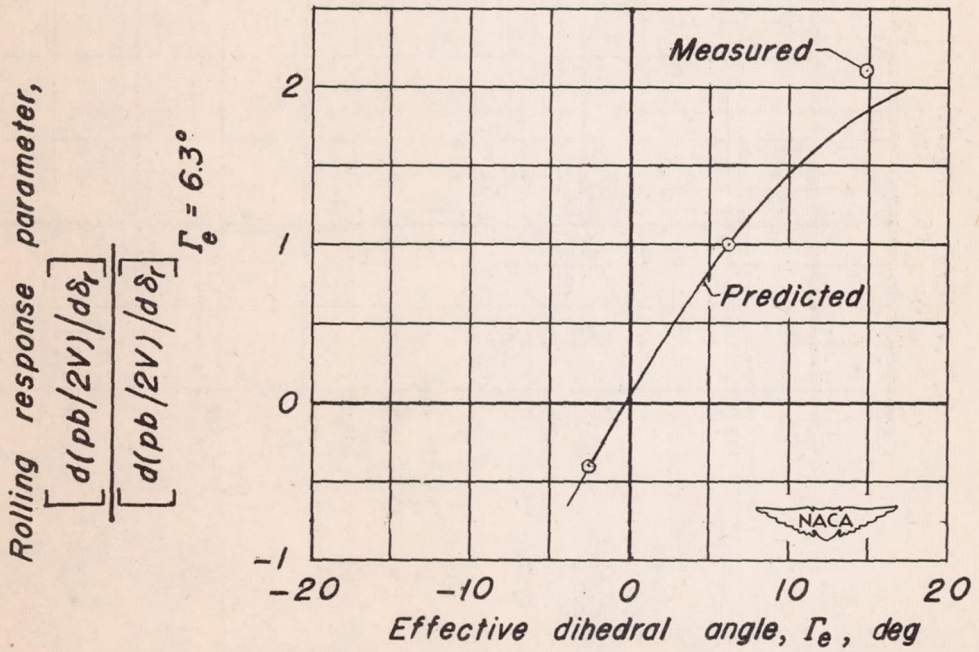

(b) Variation of rolling response parameter with Γ_e.

Figure 11.- Rolling response characteristics in abrupt rudder kicks. V_j = 350 miles per hour.

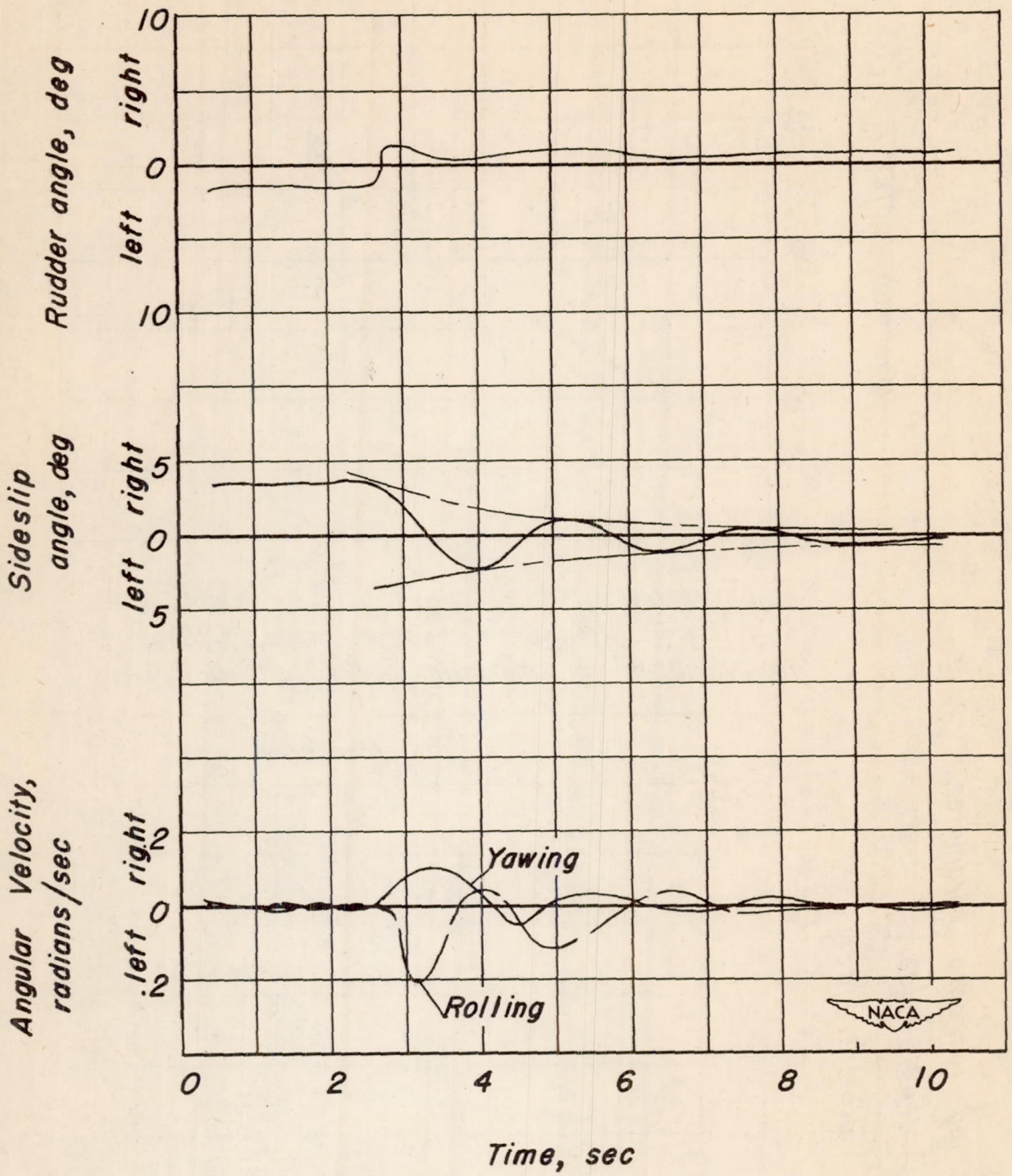

(a) Γ_e, 6.3°.

Figure 12.- Time histories of lateral oscillations. V_j = 350 miles per hour.

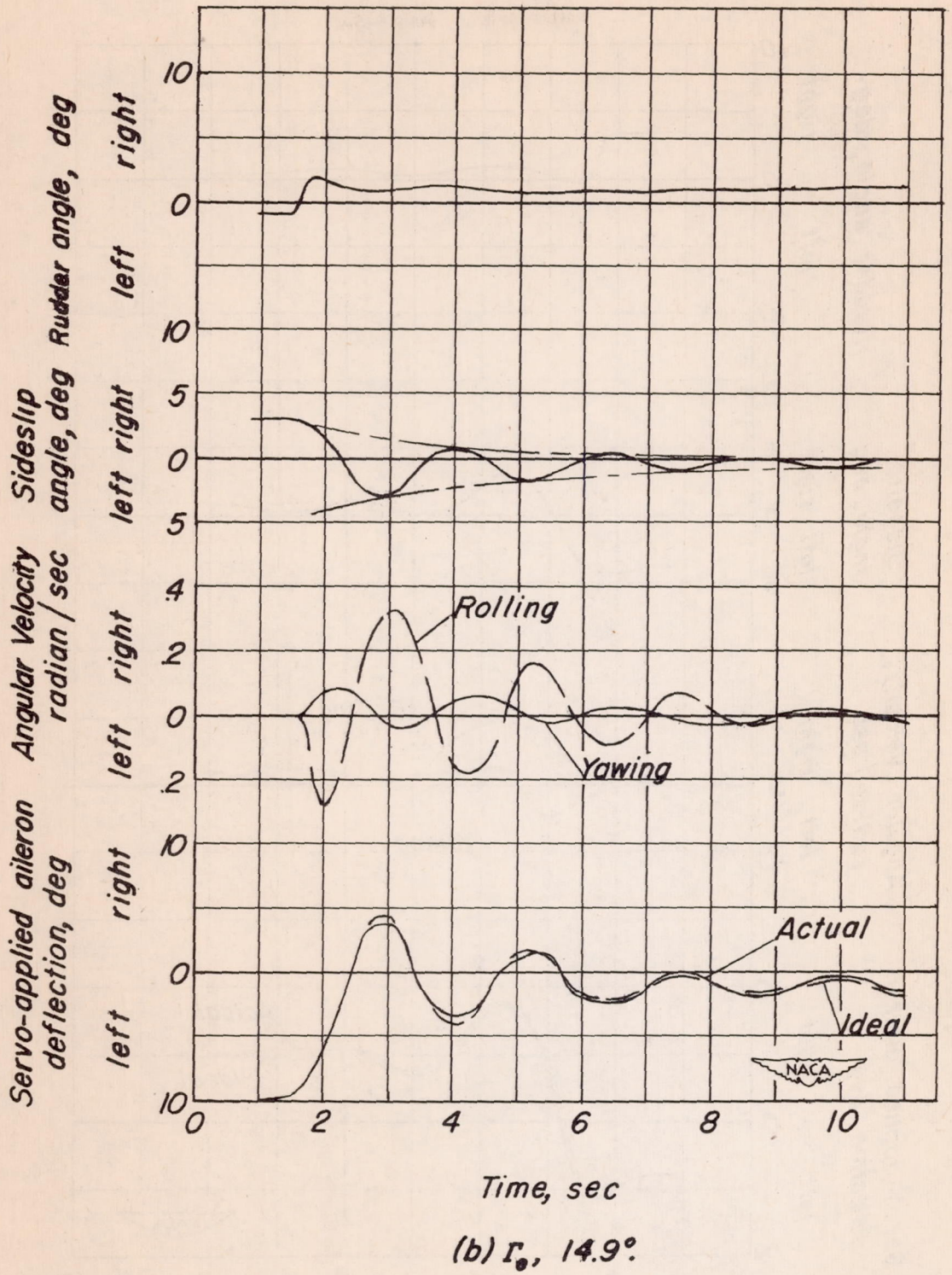

(b) Γ_o, 14.9°.

Figure 12.— Continued.

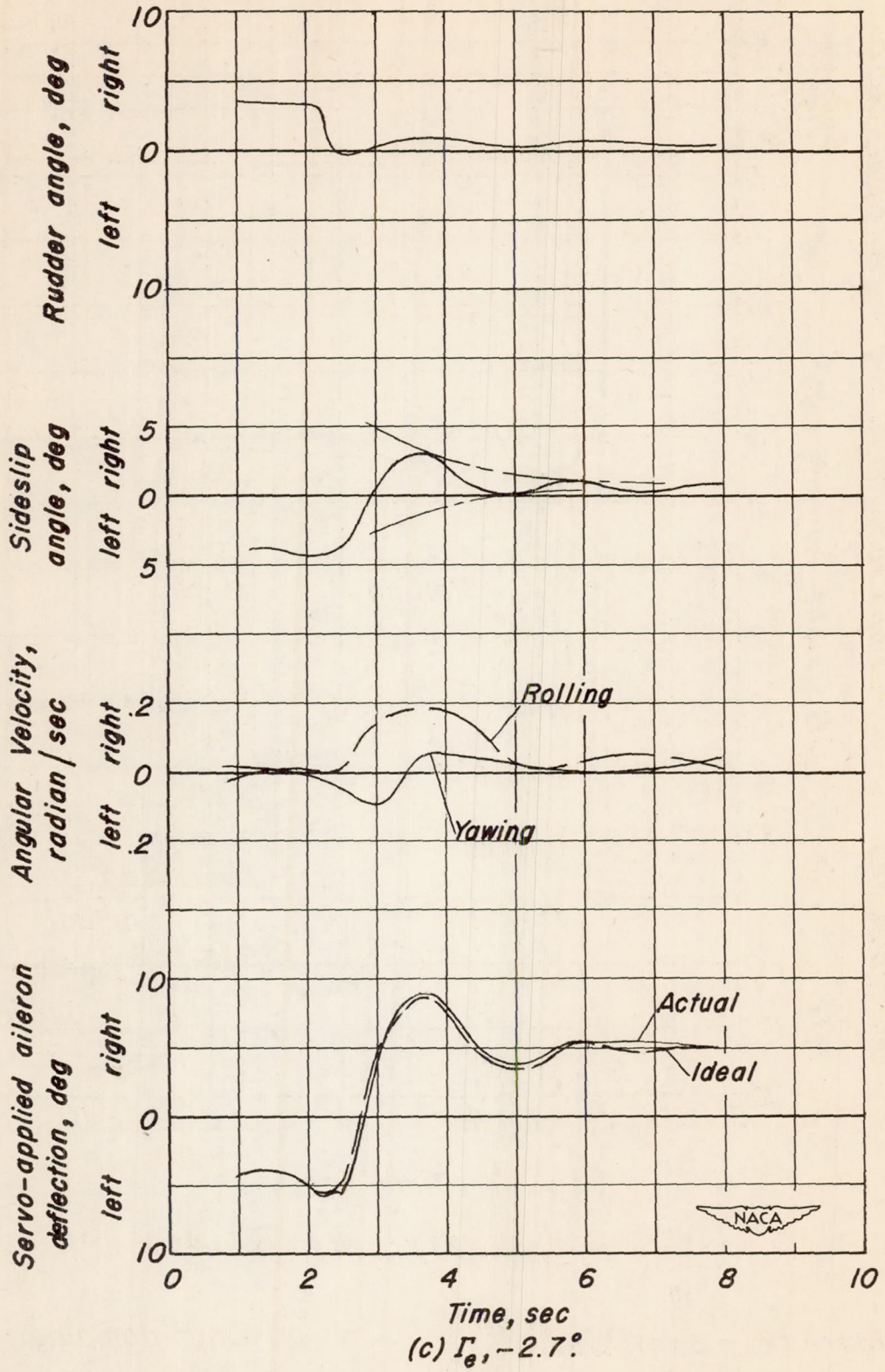

(c) Γ_e, -2.7°.

Figure 12.- Concluded.

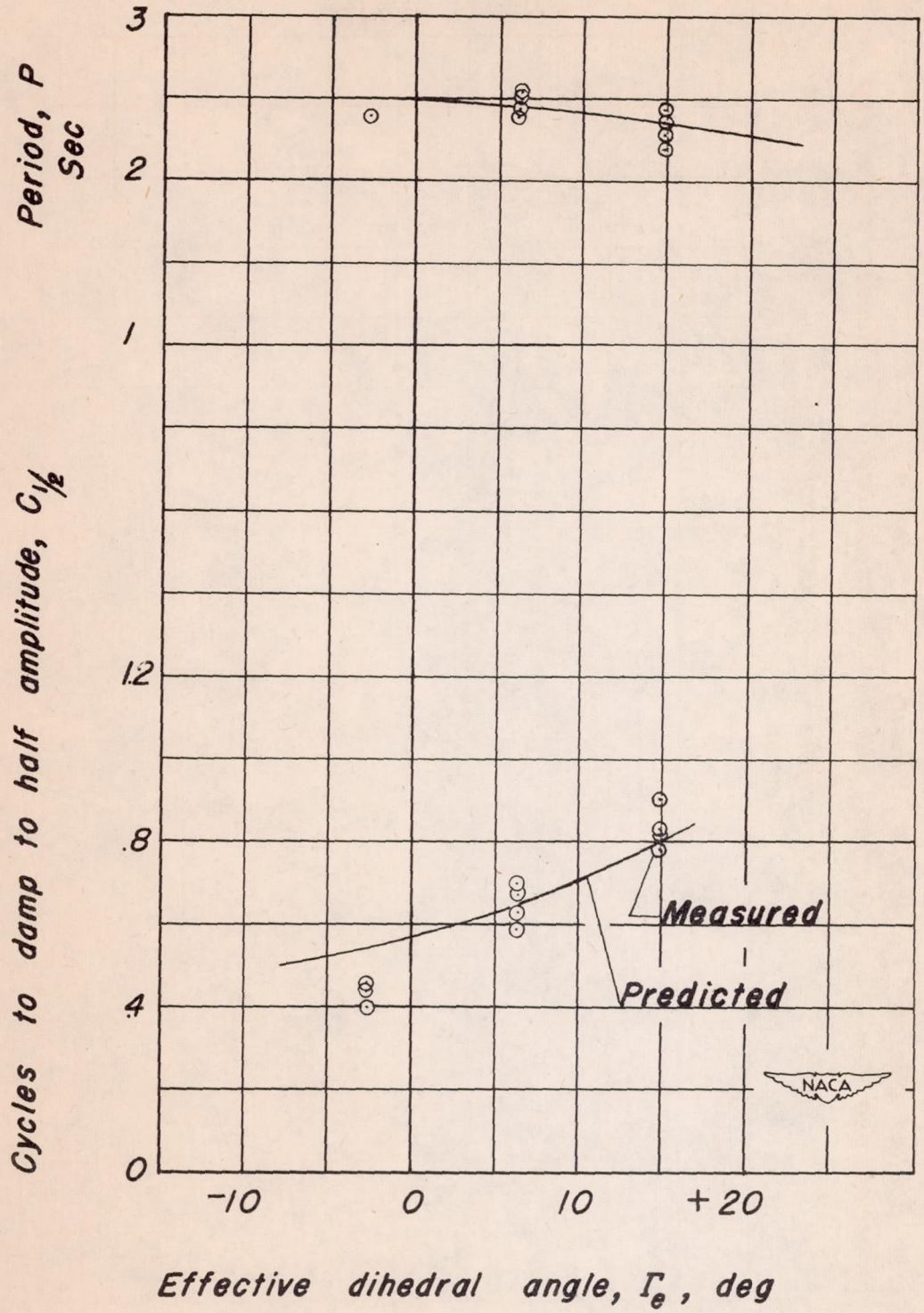

Figure 13.- Lateral-oscillation period and damping characteristics. V_i = 350 miles per hour.